Mode coupling and renormalization group results for the noisy Burgers equation

Erwin Frey
Institut für Theoretische Physik, Physik–Department der Technischen Universität München, James–Franck–Straße, D–85747 Garching, Germany

Uwe Claus Täuber *
Lyman Laboratory of Physics, Harvard University, Cambridge, MA 02138; and Institut für Theoretische Physik, Physik–Department der Technischen Universität München, James–Franck–Straße, D–85747 Garching, Germany

Terence Hwa
Physics Department, University of California at San Diego, 3500 Gilman Drive, La Jolla, CA 92093–0319

(February 1, 2008)

We investigate the noisy Burgers equation (Kardar–Parisi–Zhang equation in 1+1 dimensions) using the dynamical renormalization group (to two–loop order) and mode–coupling techniques. The roughness and dynamic exponent are fixed by Galilean invariance and a fluctuation–dissipation theorem. The fact that there are no singular two–loop contributions to the two–point vertex functions supports the mode–coupling approach, which can be understood as a self–consistent one–loop theory where vertex corrections are neglected. Therefore, the numerical solution of the mode coupling equations yields very accurate results for the scaling functions. In addition, finite–size effects can be studied. Furthermore, the results from exact Ward identities, as well as from second–order perturbation theory permit the quantitative evaluation of the vertex corrections, and thus provide a quantitative test for the mode–coupling approach. It is found that the vertex corrections themselves are of the order one. Surprisingly, however, their effect on the correlation function is substantially smaller.

PACS numbers: 05.40.+j, 64.60.Ht, 05.70.Ln, 68.35.Fx

I. INTRODUCTION

The Kardar–Parisi–Zhang (KPZ) equation represents one of the most prominent models describing nontrivial nonequilibrium dynamics [1]. This model equation constitutes one of the most thoroughly studied continuum theories of kinetic roughening. It describes the height fluctuations $h(\mathbf{x},t)$ of a stochastically grown d–dimensional interface with a growth rate $v(\boldsymbol{\nabla} h) = \lambda(\boldsymbol{\nabla} h)^2/2$ depending nonlinearly on the local orientation of the surface,

$$\frac{\partial h}{\partial t} = \nu \boldsymbol{\nabla}^2 h + \frac{\lambda}{2}(\boldsymbol{\nabla} h)^2 + \eta(\mathbf{x},t) \ . \tag{1.1}$$

The $(\nu\boldsymbol{\nabla}^2 h)$–term mimics a surface tension, and acts to smooth the interface, while the uncorrelated Langevin noise $\eta(\mathbf{x},t)$ tends to roughen the interface and entails the stochastic nature of any growth process. Its first moment vanishes, and its second moment is given by

$$\langle \eta(\mathbf{x},t)\eta(\mathbf{x}',t')\rangle = 2D\delta^{(d)}(\mathbf{x}-\mathbf{x}')\delta(t-t') \ ; \tag{1.2}$$

note that in general the coefficients ν and D are not related in any simple manner, in contrast to near–equilibrium situations where Einstein relations connect damping constants and noise correlations.

Dynamic scaling. The interface fluctuations are characteristically scale–invariant, i.e., the height profile obtained by a *self–affine rescaling* $h'(\mathbf{x},t) = b^{-\chi} h(b\mathbf{x}, b^z t)$ is, in a statistical sense, equivalent to $h(\mathbf{x},t)$. As a consequence, for sufficiently large $\mathbf{x}_0$ and t_0, such that the process is already beyond the initial transient region, the correlation function

$$C(\mathbf{x},t) = \langle [h(\mathbf{x}+\mathbf{x}_0, t+t_0) - h(\mathbf{x}_0,t_0)]^2 \rangle \tag{1.3}$$

obeys the generalized homogeneity relation ($x = |\mathbf{x}|$)

$$C(x,t) = b^{-2\chi} C(bx, b^z t) \ . \tag{1.4}$$

Upon choosing the scaling parameter $b = 1/x$ we obtain the dynamic scaling form

$$C(x,t) = x^{2\chi} \hat{C}(t/x^z) \ . \tag{1.5}$$

In the asymptotic limits $t \to 0$ and $x \to \infty$, the scaling function $\hat{C}(t/x^z)$ displays power law behavior and hence

$$C(x,t) = \begin{cases} Ax^{2\chi} & \text{for } t \to 0 \ , \\ Bt^{2\chi/z} & \text{for } x \to 0 \ . \end{cases} \tag{1.6}$$

The transverse wandering of the interface may be characterized by a perpendicular correlation length $\xi_\perp(x) \propto$

$\sqrt{C(x,t=0)} \propto x^{\chi}$ with the *roughness exponent* χ. The temporal increase of surface roughness is described by a parallel correlation length $\xi_{\parallel}(t) \propto t^{1/z}$ with the *dynamic exponent* z.

Many growth phenomena show the above dynamic scaling of the interface fluctuations, but with values for the critical exponents different from those obtained for the KPZ equation. Nevertheless, the KPZ equation has become the starting point for our understanding of nonequilibrium dynamics and strong coupling behavior.

Phenomenology of the KPZ equation. The phenomenology of the KPZ equation is now well known [2]. Below the *lower critical dimension* $d_{\rm lc} = 2$ there appear two renormalization–group (RG) fixed points, namely an infrared(IR)–unstable Gaussian fixed point and an IR–stable strong–coupling fixed point describing a smooth and a rough interface, respectively. For dimensions $d > 2$ there exists a nonequilibrium phase transition from a weak–coupling phase for small effective coupling constants $g = \lambda^2 D/\nu^3$, where the nonlinearity is irrelevant (in the RG sense), to a strong–coupling phase which seems to be inaccessible through perturbative methods [2,3]. The scaling exponents in the strong–coupling phase have been determined by numerical methods [4,5] and self–consistent mode–coupling approaches [6–8]. The results obtained from mode–coupling theory suggest the existence of an *upper critical dimension* $d_{\rm uc} = 4$ [9]. This result is supported by functional RG calculations [10,11] and renormalization group arguments [3,12]. In the numerical simulations, however, the dynamic critical exponent z for the transient roughening of an initially flat interface is found to be smaller than $z_0 = 2$ for all dimensions accessible to a numerical analysis [5], i.e., there is no indication of any upper critical dimension. This discrepancy between mode–coupling theory and numerical results has yet to be resolved and constitutes one of the most important issues of current theoretical research.

Mapping to other models. The KPZ equation is closely related to a variety of other problems ranging from fluid dynamics governed by the Burgers equation [13] to equilibrium systems with quenched disorder, namely directed polymers in random environments [14,15]. Most of these mappings and relations are strictly valid for the one–dimensional case only. In order to assist the reader with the transfer of the results obtained in the main part of this paper to related systems, we provide a short account of some of the most important issues.

The transformation $\mathbf{v} = -\boldsymbol{\nabla} h$ leads to a Langevin equation for a randomly stirred fluid

$$\frac{\partial \mathbf{v}}{\partial t} + \lambda \left(\mathbf{v}\cdot\boldsymbol{\nabla}\right)\mathbf{v} = \nu \boldsymbol{\nabla}^2 \mathbf{v} - \boldsymbol{\nabla}\eta(\mathbf{x},t) \ , \tag{1.7}$$

which in the case $\lambda = 1$ represents a d–dimensional generalization of the noisy Burgers equation [13]. The long–time and large–distance behavior of the Burgers equation, describing the dynamics of a vorticity–free velocity field, and the Navier–Stokes equation, characterizing an incompressible fluid, have been analyzed by Forster, Nelson, and Stephen in the framework of dynamical renormalization group theory to one–loop order [13]. These authors have shown that the fluctuation–dissipation theorem, valid in $d = 1$ only (see App. A), together with a Ward identity resulting from the Galilean invariance of the fluid equation of motion allow the determination of the dynamic critical exponent z in $d = 1$ to be exactly $z = 3/2$. Their RG analysis has recently been extended to two–loop order [16,2,12].

Another model of surface roughening, which is governed by the same nonlinearity as the KPZ equation, is the Kuramoto–Sivashinsky (KS) equation [17]. In contrast to the KPZ equation the KS equation is completely deterministic

$$\frac{\partial h}{\partial t} = -\nu \boldsymbol{\nabla}^2 h - \boldsymbol{\nabla}^4 h + \frac{\lambda}{2}(\boldsymbol{\nabla} h)^2 \ , \tag{1.8}$$

and is characterized by a band of unstable modes at small wave vectors. (Note that $\nu > 0$.) Numerical simulations of the discretized one—dimensional KS equation have recently demonstrated that the large–scale dynamical correlations are described by the (1+1)–dimensional KPZ equation [18]. A derivation of the KPZ equation from the KS equation has also been given in Ref. [19], where the effective parameters of the KPZ equation have been determined from the numerics of the microscopic chaotic dynamics of the KS equation. For $d \geq 2$, however, the results [20] are still controversial.

Recently, Golubović, and Wang succeeded in mapping the equilibrium statistical mechanics of a two–dimensional smectic–A liquid crystal onto the nonequilibrium dynamics of the (1+1)–dimensional stochastic nonlinear KPZ (noisy Burgers) equation [21]. Kashuba has shown that there exists a one–to–one relationship between the Hamiltonian describing the nonlinear elasticity of a two–dimensional smectic–A liquid crystal and the Hamiltonian characterizing the long–range spin fluctuations in a two–dimensional planar ferromagnet subject to (two–dimensional) dipolar forces [22]. These relationships thus provide an interesting, exact approach to study the anomalous elasticity of smectic–A liquid crystals, as well as the spin fluctuations in the ordered phase of a dipolar planar ferromagnet in two dimensions, provided the corresponding KPZ growth model can be solved exactly, or at least to a high degree of accuracy.

A number of somewhat more exotic relationships have been found very recently. E.g., the kinetics of the annihilation process $A + B \to 0$ with driven diffusion was mapped onto the (1+1)–dimensional KPZ equation [25], and the formal equivalence of the continuum limit of the Heisenberg equation of motion of a certain spin–1/2 chain with the Fokker–Planck equation corresponding to the noisy Burgers equation was demonstrated [26]. Besides these various mappings and relationships, which are valid in (1+1) dimensions only, the KPZ equation is also closely related to the dynamics of a sine–Gordon

chain [23], the driven–diffusion equation [24], and directed paths in a random media [14].

Invariances of the noisy Burgers equation. The one–dimensional KPZ equation is special in several ways. First, there is a huge list of mappings onto related models as described above. Hence any advances in understanding the growth model will have broad implications on many physical problems. Second, the noisy Burgers equation has two important "symmetry" properties, namely Galilean invariance and detailed balance. The Galilean invariance [13] of the one–dimensional hydrodynamic equation (1.7), corresponds to an invariance of the stochastic growth model with respect to an infinitesimal tilt of the surface, $h \to h + \mathbf{v}\cdot\mathbf{x}$, $\mathbf{x} \to \mathbf{x} - \lambda\mathbf{v}t$. As a consequence of this symmetry, one finds that the amplitude of the nonlinearity λ is invariant under RG transformations, which in turn implies an exponent identity relating the roughness exponent χ to the dynamic exponent z,

$$\chi + z = 2 \; . \tag{1.9}$$

Whereas the latter invariance is valid for any dimension d, the detailed balance property of the KPZ equations holds in $d = 1$ only (see Appendix A). It can be shown [1] that the Fokker–Planck equation corresponding to the (1+1)–dimensional KPZ equation has the stationary solution

$$\mathcal{P}_{\rm st}(h) \propto \exp\left[-\frac{\nu}{2D}\int dx \left(\frac{\partial h}{\partial x}\right)^2\right] \; ; \tag{1.10}$$

this implies that the roughness exponent is $\chi = 1/2$, as if the nonlinearity were entirely absent. Together with the exponent identity (1.9), one thus finds for the dynamic exponent $z = 3/2$.

Scaling of the (1+1)–dimensional KPZ equation. As a consequence of the above invariance properties of the nonlinear Langevin equation (1.1) one can show that the height–height correlation function obeys the following scaling law [27]

$$C(x,t) = Ax^{2\chi}F(\lambda\sqrt{A}t/x^z) \; . \tag{1.11}$$

The argument of the scaling function is now dimensionless, and the scaling function itself is *universal*. It acquires the asymptotic form

$$F(\xi) = \begin{cases} 1 & \text{for } \xi \to 0 \; , \\ (\xi/2g^*)^{2\chi/z} & \text{for } \xi \to \infty \; . \end{cases} \tag{1.12}$$

The RG fixed point of the (1+1)–dimensional KPZ equation turns out to be a strong–coupling fixed point. As discussed above, despite this fact the roughness and the dynamic exponent are known *exactly* as a consequence of the particular invariance properties of the one–dimensional case. The scaling function $F(\xi)$ has been calculated using a non–perturbative mode–coupling approach [27]. Striking agreement with the results of direct numerical simulations [28–30] were found.

The non–perturbative mode–coupling approach essentially consists in a resummation of the perturbation theory, such that all propagator renormalizations are properly taken into account, while the vertex corrections are neglected. This is clearly a very ad–hoc and uncontrolled procedure; nevertheless, mode–coupling theories have been remarkably successful in applications to many areas of condensed matter theory, such as structural glass transitions [31], critical dynamics of magnets [32,33], binary mixtures [32,34], and others [34]. In all those fields, it has been found that mode–coupling theory is capable of describing experiments in a quantitative manner. The factorisation approximation in the above mode coupling concepts is also known in the theory of hydrodynamic turbulence as Kraichnan's Direct Interaction Approximation [35].

The present work is motivated by this fact, and furthermore by the striking agreement of the mode–coupling results and those obtained from numerical simulations for the KPZ equation. In what follows, we will try to give a systematic analysis of the mode–coupling approach using the field–theoretic formulation of Langevin dynamics [36–38]. In particular, the fact that there are no singular two–loop contributions to the two–point vertex functions in perturbation theory in $d = 1$ strongly supports the mode–coupling approach. As the IR singularities, i.e., the exponents z and χ, are exactly known, the self–consistent treatment is expected (and found) to reproduce the scaling functions to a high degree of accuracy. In addition, we shall analyze vertex corrections in order to understand the range of validity of the mode–coupling approach. Our explicit results for the vertex corrections, as obtained from (exact) Ward identities, as well as from second–order perturbation theory allow for a quantitative estimate of the systematic errors enshrined in the mode–coupling approach. Since this specific type of self–consistent treatment is used in many areas of theoretical physics, albeit under different nomenclature, we hope that this work will shed some light on its applicability, limitations, and possible extensions.

Outline. The outline of the paper is as follows. In the subsequent section we summarize results from previous RG studies, discuss their relevance for the mode–coupling approach, and provide those explicit results which are needed in subsequent calculations. The formulation of the mode–coupling theory is discussed in Sec. III, as well as the solution of the self–consistent mode–coupling equations for the noisy Burgers equation. In addition to the scaling functions in the thermodynamic limit, finite–size corrections are explored. The size of the vertex corrections is estimated from the (exact) Ward identities stemming from Galilean invariance, as well as from the explicit two–loop perturbational contributions. In the bulk of the present work, we shall refer solely to the (1+1)–dimensional KPZ equation; however, whenever more general statements in d dimensions are possible, this restriction to $d = 1$ is relaxed. We conclude with a brief summary and a discussion of some of the

remaining open problems.

II. RESULTS FROM RENORMALIZATION GROUP THEORY

We start by reviewing some known results from perturbational renormalization group theory [1,16,2], specializing to 1+1 dimensions. This section also contains the explicit expressions for the vertex corrections to the two–point vertex functions to two–loop order. In this section, as well as in the Appendix, unrenormalized quantities are denoted by a subscript "0".

A. Dynamic functional

We start with a brief description of the field–theoretical formulation of Langevin–type dynamics [36,37]. The stochastic forces $\eta(\mathbf{x},t)$ obeying $\langle\eta(\mathbf{x},t)\rangle = 0$ and Eq. (1.2) can be taken to be Gaussian distributed,

$$W[\eta] \propto \exp\left[-\frac{1}{4D_0}\int d^dx \int dt \eta^2(\mathbf{x},t)\right] . \qquad (2.1)$$

Using the equation of motion (1.1), we can eliminate the noise term; with an additional Gaussian transformation introducing Martin–Siggia–Rose auxiliary fields $\tilde{h}$ [38] the ensuing probability distribution $P[h]$ for the height fluctuations may be further linearized, and thus the original nonlinear stochastic equation of motion can be reformulated in terms of a generating functional [2]

$$Z[j,\tilde{j}] = \int \mathcal{D}[h]\mathcal{D}[i\tilde{h}] \exp\Bigg(\mathcal{J}[\tilde{h},h] + \int d^dx \int dt \left[\tilde{j}\tilde{h} + jh\right]\Bigg) , \qquad (2.2)$$

with the Janssen–De Dominics functional given by

$$\mathcal{J}[\tilde{h},h] = \int d^dx \int dt \Bigg\{ D_0\, \tilde{h}\tilde{h} - \tilde{h}\left[\frac{\partial h}{\partial t} - \nu_0 \boldsymbol{\nabla}^2 h - \frac{\lambda_0}{2}(\boldsymbol{\nabla} h)^2\right]\Bigg\} . \qquad (2.3)$$

Correlation and response functions can now be expressed as functional averages with weight $\exp\left\{\mathcal{J}[\tilde{h},h]\right\}$. Upon separating the dynamic functional into a quadratic and a nonlinear part, a standard perturbation theory can be formulated, where the cumulants $G_{\tilde{N},N}$ of the correlation and response functions are defined by functional derivatives of $F[\tilde{j},j] = \ln Z[\tilde{j},j]$ with respect to the sources $\tilde{j}$ and j, respectively. Vertex functions $\Gamma_{\tilde{N},N}$ are then obtained from the cumulants by a Legendre transformation,

$$\Gamma[\tilde{h},h] = -F[\tilde{j},j] + \int d^dx \int dt (\tilde{h}\tilde{j} + hj) , \qquad (2.4)$$

where

$$h = \delta F/\delta j , \quad \text{and} \quad \tilde{h} = \delta F/\delta \tilde{j} . \qquad (2.5)$$

We finally note that the functional determinant originating in the variable change from the noise fields η to the height fluctuations h serves to exactly cancel the acausal contributions to the perturbation series, thus leaving only those Feynman diagrams with correct time ordering in the response propagators [36,2].

B. Two–point Vertex functions and renormalization

We can now proceed to study the renormalization of the KPZ equation in one dimension. As discussed in detail in Ref. [2], the Ward identity stemming from the Galilean invariance of the Burgers equation shows that the nonlinearity $\lambda = \lambda_0$ does not renormalize. This leaves the renormalization of the surface tension (diffusion coefficient) ν_0 and of the noise correlation strength D_0, which may be inferred from studying the two–point vertex functions $\partial_{q^2}\Gamma_{\tilde{h}h}(q,\omega)$ and $\Gamma_{\tilde{h}\tilde{h}}(q,\omega)$, respectively; because of the fluctuation–dissipation theorem valid (only) in $d = 1$ (see Appendix A), these coefficients are actually proportional to each other and must therefore renormalize in the same way. In Appendix B, we list the Feynman diagrams and the corresponding analytical expressions for $\Gamma_{\tilde{h}h}(q,\omega)$ to two–loop order (second–order perturbation theory in λ), specializing the results of Ref. [2] to $d = 1$. Upon collecting these terms, splitting the vertex functions into regular and (UV) singular parts, $\Gamma_{\tilde{h}h} = \Gamma^{reg}_{\tilde{h}h} + \Gamma^{sing}_{\tilde{h}h}$, eventually the following comparatively simple results are obtained:

$$\frac{\Gamma^{\rm reg}_{\tilde{h}h}(q,\omega)}{i\omega + \nu_0 q^2} = -\frac{\lambda^4 D_0^2}{2\nu_0^3} q^2 \int_p\int_k \frac{q_-}{i\omega + \nu_0 q_+^2 + \nu_0 q_-^2} \times \times \frac{1}{\tilde{q}_-[i\omega + \nu_0\tilde{q}_+^2 + \nu_0\tilde{q}_-^2][i\omega + \nu_0 q_+^2 + \nu_0\tilde{q}_-^2 + \nu_0 k^2]} \qquad (2.6)$$

$$\Gamma^{\rm sing}_{\tilde{h}h}(q,\omega) = i\omega + \nu_0 q^2 + \frac{\lambda^2 D_0}{2\nu_0} q^2 \int_p \frac{1}{i\omega + \nu_0 q_+^2 + \nu_0 q_-^2} ; \qquad (2.7)$$

here we have introduced the abbreviations $q_\pm = (q/2) \pm p$, $\tilde{q}_\pm = q_\pm \pm k$, and $\int_p = \int_{-\infty}^{+\infty} dp/2\pi$. Note that the singular term stems entirely from the one–loop diagram (the expression involving only one internal momentum p), while the (UV) singular two–loop contribution vanishes. The second–order term in the perturbation expansion thus yields merely regular corrections to the scaling functions. The second relevant vertex function can be written as $\Gamma_{\tilde{h}\tilde{h}}(q,\omega) = -2D_0 {\rm Re}\Gamma_{\tilde{h}h}(q,\omega)/\nu_0 q^2$, which allows us to define the wavenumber– and frequency–dependent diffusion coefficient as

$$\nu(q,\omega) = \frac{1}{\nu_0 q^2}\mathrm{Re}\Gamma_{\tilde{h}h}(q,\omega) = -\frac{1}{2D_0}\Gamma_{\tilde{h}\tilde{h}}(q,\omega) \ , \quad (2.8)$$

confirming the validity of the fluctuation–dissipation theorem of Appendix A [2,16].

In evaluating those contributions which become singular as the critical dimension $d_{\rm lc} = 2$ is approached, one has to be careful to choose a normalization point (NP) where either q or ω are finite, in order not to interfere with the IR singularities, which would also appear as poles in $\varepsilon = d - 2$ (for a more detailed discussion, see Refs. [2] and [12]). A convenient choice is NP: $q = \mathbf{0}$, $i\omega/2\nu = \kappa^2$; with $g_0 = \lambda^2 D_0/\nu_0^3$ one thus arrives at

$$\Gamma_{\tilde{h}\tilde{h}}(q,\omega)^{\rm sing}_{\rm NP} = -2D_0\left[1+\frac{g_0}{4}\int_p \frac{1}{\kappa^2 Z + p^2}\right] , \quad (2.9)$$

$$\frac{\partial}{\partial q^2}\Gamma_{\tilde{h}h}(q,\omega)^{\rm sing}_{\rm NP} = \nu_0\left[1+\frac{g_0}{4}\int_p \frac{1}{\kappa^2 Z + p^2}\right] , \quad (2.10)$$

where Z is the renormalization factor for both ν and D. The remaining singular integral is readily evaluated using the dimensional regularization scheme

$$\int_p \frac{1}{\mu^2 + p^2} = -\frac{C_d \mu^\varepsilon}{\varepsilon} \ , \quad (2.11)$$

where $C_d = \Gamma(2 - d/2)/2^{d-1}\pi^{d/2}$ is a geometry factor, and $C_1 = 1/2$. Note that in this evaluation at *fixed* dimension $d = 1$, no expansion with respect to $\varepsilon = d - 2$ was applied; the latter parameter was merely used to effectively count the singularities in the integrals that would appear at $d_{\rm lc} = 2$, when they are generalized to arbitrary dimension d. These ultraviolet (UV) poles may now be absorbed in renormalized quantities $D = ZD_0$ and $\nu = Z\nu_0$, with the renormalization constant

$$Z = 1 - \frac{g_0\kappa^\varepsilon}{8\varepsilon} + \frac{g_0^2\kappa^{2\varepsilon}}{128\varepsilon} \ . \quad (2.12)$$

Defining the renormalized coupling

$$g = \frac{g_0}{Z^2\kappa} \ , \quad (2.13)$$

we can now readily calculate Wilson's flow functions,

$$\zeta(g) = \kappa\partial_\kappa|_0 \ln Z = -g/8 \, , \quad (2.14)$$

$$\beta(g) = \kappa\partial_\kappa|_0 g = g(d - 2 - 2\zeta) = g(-1 + g/4) \quad (2.15)$$

in $d = 1$. Searching for zeros of the beta function yields the (IR) stable nontrivial fixed point

$$g^* = 4 \ , \quad (2.16)$$

from which the critical exponents

$$\chi = -\zeta(g^*) = 1/2 \ , \quad (2.17)$$

$$z = 2 + \zeta(g^*) = 3/2 \quad (2.18)$$

can be deduced. Note that these explicit results fulfill the exponent sum rule (1.9); of course, as these exponents can already be determined from this identity and the additional constraint of the fluctuation–dissipation theorem (see Appendix A), this rather serves as a check for the calculations. Note that the remarkable cancellation of the singulartwo-loop contributions has been essential here from the diagrammatic point of view.

In Ref. [2], the renormalization group approach is carried out in arbitrary space dimension $0 \le d < 4$. For $d > 2$ an expansion with respect to $\varepsilon = d - 2$ can be pursued, and was in fact recently carried through to arbitrary order in the perturbation series by Lässig [3]. For $d < 2$, on the other hand, one may note that the fixed point coupling $g^* \propto d$ approaches zero for $d \to 0$, and the results may be cast into an expansion about zero space dimension [12].

C. Two–loop scaling functions

For later use, we now summarize the results from the second–order perturbation theory once more, albeit with some slight changes. First, we explicitly separate the zero– and one–loop contributions, and the two-loop contributions due to propagator and vertex renormalizations. Second, we take "self–consistent" propagators, i.e., we generalize ν_0 and D_0 to a q–dependent quantity according to Eq. (2.8), however neglecting its frequency dependence. This is in the spirit of the Lorentzian approximation in mode–coupling theory, to be discussed below; its formal advantage is that the pole structure in the complex frequency plane remains unaltered, and therefore the results from Appendix B may be readily generalized. The zero– and one–loop contributions to $\Gamma_{\tilde{h}h}(q,0)$ thus read (see Fig. 7a,b):

$$\Gamma^{(1)}_{\tilde{h}h}(q,0) = q^2\left[\nu(q) + \frac{\lambda^2}{2}\int_p \frac{1}{\nu(q_+)q_+^2 + \nu(q_-)q_-^2}\right] \ ; \quad (2.19)$$

similarly, the two–loop contribution due to propagator renormalization (Fig. 7c–f) becomes

$$\Gamma^{(2,\rm p)}_{\tilde{h}h}(q,0) = -q^2\frac{\lambda^4}{2}\int_p\int_k \frac{q_-^2}{[\nu(q_+)q_+^2 + \nu(q_-)q_-^2]^2} \times \frac{1}{\nu(q_+)q_+^2 + \nu(\bar{q}_+)\bar{q}_+^2 + \nu(\bar{q}_-)\bar{q}_-^2} \ , \quad (2.20)$$

while the result for the two–loop contribution due to vertex corrections (Fig. 7g–j) is

$$\Gamma^{(2,\rm v)}_{\tilde{h}h}(q,0) = -q^2\lambda^4\int_p\int_k \frac{q_-}{\nu(q_+)q_+^2 + \nu(q_-)q_-^2} \times \frac{\tilde{q}_+}{[\nu(\tilde{q}_+)\tilde{q}_+^2 + \nu(\tilde{q}_-)\tilde{q}_-^2][\nu(q_+)q_+^2 + \nu(\tilde{q}_-)\tilde{q}_-^2 + \nu(k)k^2]} \ . \quad (2.21)$$

III. MODE COUPLING THEORY AND VERTEX CORRECTIONS

In this section we study the mode coupling approximation for the Burgers equation. For readers not familiar with the dynamical functional approach discussed in the previous section, we start by a derivation of the mode coupling equation using a perturbation theory for the equation of motion.

A. Perturbation series and mode coupling equations

In Fourier space with the equation of motion (1.1) reads

$$h(\mathbf{k},\omega) = G_0(\mathbf{k},\omega)\eta(\mathbf{k},\omega) + G_0(\mathbf{k},\omega)\widetilde{j}(\mathbf{k},\omega) + \frac{1}{2}G_0(\mathbf{k},\omega)\int_{\mathbf{q},\mu} V^{(0)}_{\mathbf{k}_+;\mathbf{k}_-} h(\mathbf{k}_+,\omega_+)h(\mathbf{k}_-,\omega_-) \ . \tag{3.1}$$

where $G_0(\mathbf{k},\omega) = 1/(\nu\mathbf{k}^2 - i\omega)$ is the "bare propagator", $V^{(0)}_{\mathbf{k}_1;\mathbf{k}_2} = -\lambda\,\mathbf{k}_1\cdot\mathbf{k}_2$ is the "bare vertex", and $\mathbf{k}_\pm \equiv \mathbf{k}/2 \pm \mathbf{q}$, $\omega_\pm \equiv \omega/2 \pm \mu$. The noise η is assumed to be Gaussian and uncorrelated, given by the weight function Eq. (2.1). A small external perturbation $\widetilde{j}(\mathbf{k},\omega)$ has also been included in Eq. (3.1), and will be used to generate the response functions. Typically, the quantities of interest are the noise–averaged two–point correlation function

$$\langle h(\mathbf{K})h(\mathbf{K}')\rangle = C(\mathbf{K})\delta(\mathbf{K}+\mathbf{K}') \ , \tag{3.2}$$

and the noise–averaged linear response function

$$\left\langle \frac{\delta h(\mathbf{K})}{\delta\widetilde{j}(\mathbf{K}')}\right\rangle = G(\mathbf{K})\delta(\mathbf{K}-\mathbf{K}') \ , \tag{3.3}$$

where $(\mathbf{k},\omega)$ is abbreviated by $\mathbf{K}$ and $\delta(\mathbf{K}+\mathbf{K}') = (2\pi)^{d+1}\delta^d(\mathbf{k}+\mathbf{k}')\delta(\omega+\omega')$. These are special cases of the general Green's function

$$G_{m,n}(-\mathbf{P}_1;\ldots;-\mathbf{P}_m|\mathbf{K}_1;\ldots;\mathbf{K}_n) = \left\langle \frac{\delta^m(h(\mathbf{K}_1)\cdots h(\mathbf{K}_n))}{\delta\widetilde{j}(\mathbf{P}_1)\cdots\delta\widetilde{j}(\mathbf{P}_m)}\right\rangle_c \ , \tag{3.4}$$

where the subscript "c" denotes the connected part. In this notation, the two–point correlation function is $\langle h(\mathbf{K})h(\mathbf{K}')\rangle = G_{0,2}(\cdot|\mathbf{K};\mathbf{K}')$ and the linear response function is $\langle \delta h(\mathbf{K})/\delta\widetilde{j}(\mathbf{K}')\rangle = G_{1,1}(-\mathbf{K}'|\mathbf{K})$. From Eq. (3.4), it is clear that $G_{m,0} = 0$. The above definition of the Green's functions is identical to the one used in the dynamic functional formalism (Sec. II A).

One approach to study the Green's functions $G_{m,n}$ is perturbation theory. For $V^{(0)} = 0$, Eq. (3.1) is just the linear diffusion equation. For $V^{(0)} \neq 0$, the solution of Eq. (3.1) may be obtained iteratively by a perturbation expansion in powers of $V^{(0)}$. For example, the lowest order correction to the response function is

$$G_1(\mathbf{K}) = G_0(\mathbf{K}) + G_0(\mathbf{K})\Sigma_1(\mathbf{K})G_0(\mathbf{K}) \ , \tag{3.5}$$

where $C_0(\mathbf{K}) = 2D|G_0(\mathbf{K})|^2$ is the "bare correlator", and

$$\Sigma_1(\mathbf{K}) = -\int_{\mathbf{Q}} V^{(0)}_{\mathbf{k}_+;\mathbf{k}_-} G_0(\mathbf{K}_-)C_0(\mathbf{K}_+)V^{(0)}_{\mathbf{k}_+;\mathbf{k}} \tag{3.6}$$

is the one–loop renormalization of the "self–energy". Similarly, the lowest order correction to the correlation function is

$$C_1(\mathbf{K}) = 2D_1(\mathbf{K})|G_0(\mathbf{K})|^2 \ , \tag{3.7}$$

where

$$D_1(\mathbf{K}) = D + \frac{1}{4}\int_{\mathbf{Q}} V^{(0)}_{\mathbf{k}_+;\mathbf{k}_-} C_0(\mathbf{K}_-)C_0(\mathbf{K}_+)V^{(0)}_{\mathbf{k}_+;\mathbf{k}_-} \tag{3.8}$$

is the one–loop renormalization of the "noise spectrum". Unfortunately, such perturbation series diverge in the hydrodynamic limit $\mathbf{k},\omega \to 0$. One way to proceed is to perform a renormalization group analysis. It turns out, however, that there is no fixed point that can be obtained in a controlled ε expansion with $\varepsilon = 2-d$ below $d = 2$ dimensions [2]. Hence, a non–perturbative method is required to treat the KPZ problem. One approximation which has been frequently used is to replace the bare propagator G_0 and bare correlator C_0 in Eqs. (3.6) and (3.8) by the renormalized functions G and C while keeping the vertex $V^{(0)}$ unchanged. This is known as the mode–coupling approximation (or Kraichnan's Direct Interaction Approximation), and it leads to the following closed set of integral equations,

$$\Sigma(\mathbf{K}) = -\int_{\mathbf{Q}} V^{(0)}_{\mathbf{k}_+;\mathbf{k}_-} G(\mathbf{K}_-)C(\mathbf{K}_+)V^{(0)}_{\mathbf{k}_+;\mathbf{k}} \ , \tag{3.9}$$

$$D(\mathbf{K}) = D + \frac{1}{4}\int_{\mathbf{Q}} V^{(0)}_{\mathbf{k}_+;\mathbf{k}_-} C(\mathbf{K}_-)C(\mathbf{K}_+)V^{(0)}_{\mathbf{k}_+;\mathbf{k}_-} \ , \tag{3.10}$$

where Σ and D are defined by G and C through

$$G^{-1}(\mathbf{K}) = G_0^{-1}(\mathbf{K}) - \Sigma(\mathbf{K}), \tag{3.11}$$

$$C(\mathbf{K}) = 2D(\mathbf{K})|G(\mathbf{K})|^2 \ . \tag{3.12}$$

Of course, as this procedure neglects any vertex renormalizations, it constitutes a partial sum of the perturbation series only, and as a–priori no information is available about the size of the missing contributions, it clearly constitutes an uncontrolled approximation. Nevertheless, the mode coupling theory has been quite successfully applied in many areas of condensed matter theory, as mentioned in the introduction. It was first applied to the KPZ problem by van Beijeren, Kutner, and Spohn [24] to get the scaling exponents χ and z in $d = 1$. Recently, the mode–coupling equations were solved numerically to obtain the entire function $C(\mathbf{k},\omega)$ in $1+1$ dimensions [27], and striking agreement to the scaling function obtained by direct numerical simulations [28] were found (for details see Sec. III C below). This result is very surprising and prompted us to study the mode–coupling theory in more detail. In what follows, we will try to give a systematic analysis of the mode–coupling approach using the field–theoretic formulation of Langevin dynamics.

B. Dynamic field theory, Ward identities, and vertex corrections

The starting point of our study is the response function, which can be formally obtained by differentiating Eq. (3.1) with respect to the perturbation $\widetilde{j}(\mathbf{K}')$. We obtain

$$G_{1,1}(-\mathbf{K}'|\mathbf{K}) = G_0(\mathbf{K})\delta(\mathbf{K}-\mathbf{K}') + \frac{1}{2}G_0(\mathbf{K})\int_{\mathbf{Q}} V^{(0)}_{\mathbf{k}_+;\mathbf{k}_-} G_{1,2}(-\mathbf{K}'|\mathbf{K}_+;\mathbf{K}_-) \ . \tag{3.13}$$

Mode coupling theory amounts to expressing $G_{1,2}$ in terms of the lower order functions $G_{1,1}$ and $G_{0,2}$.

In order to analyze the Green's functions systematically, we turn to a functional integral method described in section II. From the generating functional, Eq. (2.2) the Green's functions, Eq. (3.4), can be easily obtained as the functional derivatives of $F[\widetilde{j},j] = \log Z[\widetilde{j},j]$.

By taking derivatives of Eqs. (2.5) and using Eq. (2.4), it is straightforward to relate the Green's functions $G_{m,n}$ to the vertex function $\Gamma_{m,n}$'s, e.g.,

$$\Gamma_{1,1}(\mathbf{P}|\mathbf{K}) = \Gamma_{1,1}(-\mathbf{P}) = G^{-1}(\mathbf{P})\delta(\mathbf{K}+\mathbf{P}) \ . \tag{3.14}$$

The two–point correlation function can also be easily found. It has the form of Eq. (3.12), with

$$\Gamma_{2,0}(\mathbf{P}_1,\mathbf{P}_2|\cdot) = \Gamma_{2,0}(\mathbf{P}_1) = -2D(\mathbf{P}_1)\delta(\mathbf{P}_1+\mathbf{P}_2) \ . \tag{3.15}$$

All higher order Green's functions can be written as products of $G(\mathbf{K})$, $C(\mathbf{K})$, and the higher order vertex functions. For example,

$$G_{2,1}(\mathbf{P}_1;\mathbf{P}_2|\mathbf{K}) = -G(\mathbf{K})\,\Gamma_{1,2}(\mathbf{K}|\mathbf{P}_1;\mathbf{P}_2)\,G(-\mathbf{P}_1)G(-\mathbf{P}_2) \ , \tag{3.16}$$

$$\begin{aligned} G_{1,2}(\mathbf{P}|\mathbf{K}_1;\mathbf{K}_2) = &-G(\mathbf{K}_1)G(\mathbf{K}_2)\,\Gamma_{2,1}(\mathbf{K}_1;\mathbf{K}_2|\mathbf{P})\,G(-\mathbf{P}) \\ &-G(\mathbf{K}_1)C(\mathbf{K}_2)\,\Gamma_{1,2}(\mathbf{K}_1|\mathbf{K}_2;\mathbf{P})\,G(-\mathbf{P}) \\ &-C(\mathbf{K}_1)G(\mathbf{K}_2)\,\Gamma_{1,2}(\mathbf{K}_2|\mathbf{K}_1;\mathbf{P})\,G(-\mathbf{P}) \ . \end{aligned} \tag{3.17}$$

Using Eq. (3.17) in Eq. (3.13), we obtain

$$\begin{aligned} G_{1,1}(-\mathbf{K}'|\mathbf{K}) &= G(\mathbf{K})\delta(\mathbf{K}-\mathbf{K}') \\ &= G_0(\mathbf{K})\delta(\mathbf{K}-\mathbf{K}') - G_0(\mathbf{K})\int_{\mathbf{Q}} V^{(0)}_{\mathbf{k}_+;\mathbf{k}_-} G(\mathbf{K}_-) \\ &\times\left[C(\mathbf{K}_+)\Gamma_{1,2}(\mathbf{K}_-|\mathbf{K}_+;-\mathbf{K}') + \frac{1}{2}G(\mathbf{K}_+)\Gamma_{2,1}(\mathbf{K}_-;\mathbf{K}_+|-\mathbf{K}')\right]G(\mathbf{K}') \end{aligned} \tag{3.18}$$

for the full response function. Note that it has the form $G(\mathbf{K}) = G_0(\mathbf{K}) + G_0(\mathbf{K})\Sigma(\mathbf{K})G(\mathbf{K})$, where $\Sigma(\mathbf{K})$ is the self energy defined in Eq. (3.11). If we write the vertex functions as

$$\Gamma_{1,2}(\mathbf{K}|\mathbf{K}_1;\mathbf{K}_2) = \Gamma_a(\mathbf{K}_1;\mathbf{K}_2)\delta(\mathbf{K}+\mathbf{K}_1+\mathbf{K}_2) \ , \tag{3.19}$$

$$\Gamma_{2,1}(\mathbf{P}_1;\mathbf{P}_2|\mathbf{K}) = \Gamma_b(\mathbf{P}_2;\mathbf{K})\delta(\mathbf{K}+\mathbf{P}_1+\mathbf{P}_2) \ , \tag{3.20}$$

then the self–energy becomes

$$\Sigma(\mathbf{K}) = -\int_{\mathbf{Q}} V^{(0)}_{\mathbf{k}_+;\mathbf{k}_-} G(\mathbf{K}_-)C(\mathbf{K}_+)V(\mathbf{K}_+;\mathbf{K}) \ , \tag{3.21}$$

where

$$V(\mathbf{K}_+;\mathbf{K}) = \Gamma_a(\mathbf{K}_+;-\mathbf{K}) + \frac{G^{-1}(-\mathbf{K}_+)}{4D(\mathbf{K}_+)}\Gamma_b(\mathbf{K}_+;-\mathbf{K}) \tag{3.22}$$

denotes the "renormalized vertex function". It will be useful to write the vertex function in a slightly different form,

$$V(\mathbf{K}_+;\mathbf{K}) = \Gamma_a(\mathbf{K}_+;-\mathbf{K}) + \frac{G^{-1}(\mathbf{K}_+)+G^{-1}(-\mathbf{K}_+)}{4D(\mathbf{K}_+)}\Gamma_b(\mathbf{K}_+;-\mathbf{K}) \ . \tag{3.23}$$

The additional term does not change $\Sigma(\mathbf{K})$ in Eq. (3.21) because its poles, from $G(\mathbf{K}_-)$ and $G(-\mathbf{K}_+)$, are on the same side of the complex frequency plane. Hence the frequency integral for this additional term yields zero. Comparing Eq. (3.21) with Eq. (3.9), we realize that the mode–coupling equation becomes exact if $V(\mathbf{K}_+;\mathbf{K}) = V^{(0)}_{\mathbf{k}_+;\mathbf{k}}$. In section III D, we will show that this equality in fact does not hold. Yet, by exploiting a number of identities relating the different vertex functions, we shall show that the correction to $V(\mathbf{K}_+;\mathbf{K})$ is small in the limit $\mathbf{K}\to 0$. This is hopefully the first step in understanding the puzzle of why the mode coupling theory works so well, at least in the case of the noisy Burgers equation.

C. Numerical solution of the mode coupling equations

In this section we present the numerical solution of the (1+1)–dimensional KPZ equation. In view of the results

from the preceding section it is convenient to define a generalized kinetic coefficient $D(k,\omega)$ and a generalized "surface tension" $\nu(k,\omega)$ by

$$G(k,\omega) = \frac{1}{-i\omega + \nu(k,\omega)} \ , \tag{3.24}$$

$$C(k,\omega) = \frac{2D(k,\omega)}{\omega^2 + [\nu(k,\omega)]^2} \ . \tag{3.25}$$

Then, the self-consistent equations for the correlation function $C(k,\omega)$ and the response function $G(k,\omega)$ in Fourier space are given by

$$\nu(k,\omega) = \lambda^2 \int_{q,\mu} k_+^2 k k_- C(k_+,\omega_+) G(k_-,\omega_-) \ , \tag{3.26}$$

$$D(k,\omega) = \frac{\lambda^2}{4} \int_{q,\mu} k_+^2 k_-^2 C(k_+,\omega_+) C(k_-,\omega_-) \ . \tag{3.27}$$

For the numerical solution of the mode–coupling equations it is much more convenient to study the intermediate correlation and response functions, defined by full or half–sided Fourier transforms, respectively,

$$C(k,\omega) = \int_{-\infty}^{\infty} dt e^{i\omega t} C(k,t) \ , \tag{3.28}$$

$$G(k,\omega) = \int_{-\infty}^{\infty} dt e^{i\omega t} \Theta(t) G(k,t) \ . \tag{3.29}$$

Inserting into Eqs. (3.26)–(3.27) we get for the generalized kinetic coefficients

$$\nu(k,t) = \lambda^2 \int_q k_+^2 k k_- C(k_+,t) G(k_-,t) \ , \tag{3.30}$$

$$D(k,t) = \left(\frac{\lambda}{2}\right)^2 \int_q k_+^2 k_-^2 C(k_+,t) C(k_-,t) \ , \tag{3.31}$$

where

$$D(k,\omega) = \int_{-\infty}^{\infty} dt e^{i\omega t} D(k,t) \ , \tag{3.32}$$

$$\nu(k,\omega) = \int_{-\infty}^{\infty} dt e^{i\omega t} \Theta(t) \nu(k,t) \ . \tag{3.33}$$

It is again important to realize that for the (1+1)–dimensional KPZ equation there exists a fluctuation–dissipation theorem (FDT) which relates the generalized kinetic coefficient $D(k,t)$ with the generalized surface tension $\nu(k,t)$. As shown in Appendix A (see Eq. (A11)), the following identity holds

$$G(k,t) = \frac{\nu k^2}{D} \Theta(t) C(k,t) \ . \tag{3.34}$$

This allows one to rewrite $\nu(k,t)$ as

$$\nu(k,t) = k^2 \frac{\lambda^2 D}{2\nu} \int_q G(k_+,t) G(k_-,t) \, . \tag{3.35}$$

Together with Eq. (3.24), which can be written as

$$\frac{\partial}{\partial t} G(k,t) = -\int_0^t d\tau \nu(k,\tau) G(k,t-\tau) \, , \tag{3.36}$$

one now has a set of self–consistent equations for the effective surface tension and the response function.

Scaling analysis of the mode coupling equations. We look for the solutions of the scaling form

$$\nu(k,\omega) = \bar{\lambda} \nu k^z \hat{\nu}(\hat{\omega}) \ , \tag{3.37}$$

$$D(k,\omega) = \bar{\lambda} D k^{-\mu} \hat{\nu}(\hat{\omega}) \ , \tag{3.38}$$

where we have defined the scaling variable $\hat{\omega} = \omega/\bar{\lambda}\nu k^z$. The corresponding scaling forms for the Fourier–transformed quantities read

$$\nu(k,t) = \left(\bar{\lambda}\nu k^z\right)^2 \hat{\nu}(\hat{t}) \ , \tag{3.39}$$

$$D(k,t) = \bar{\lambda}^2 D \nu k^{z-\mu} \hat{\nu}(\hat{t}) \ , \tag{3.40}$$

with the scaling variable $\hat{t} = \bar{\lambda}\nu k^z t$. For the response function the scaling analysis leads to

$$G(k,\omega) = \frac{1}{\bar{\lambda}\nu k^z} \hat{G}(\hat{\omega}) \ , \tag{3.41}$$

$$G(k,t) = \hat{G}(\hat{t}) \ . \tag{3.42}$$

Inserting the scaling forms, Eqs. (.3.37)–(3.40), into the mode–coupling equations implies for the dynamic exponent $z = 3/2$, and leads to the following self–consistency equations for the generalized kinetic coefficient and the response function:

$$\hat{\nu}(\hat{t}) = \frac{1}{2\pi} \int_0^{\infty} dx \hat{G}(x_+\hat{t}) \hat{G}(x_-\hat{t}) \ , \tag{3.43}$$

$$\frac{\partial}{\partial t} \hat{G}(\hat{t}) = -\int_0^{\hat{t}} d\hat{\tau} \hat{\nu}(\hat{\tau}) \hat{G}(\hat{t}-\hat{\tau}) \ , \tag{3.44}$$

where $x_\pm = 1/2 \pm x$, and the effective coupling constant is given by

$$\bar{\lambda}^2 = \lambda^2 D/\nu^3 \ . \tag{3.45}$$

Note that the amplitude $\bar{\lambda}$ is arbitrary. We have chosen it to be equal to the effective coupling constant in order to simplify the scaled mode–coupling equations.

It can be shown analytically from Eq. (3.43) that the scaling function for the generalized surface tension $\hat{\nu}(\hat{t})$ shows a power–law behavior $\hat{\nu}(\hat{t}) = \bar{\nu}\hat{t}^{-2/3}$ with $\bar{\nu} \approx 0.1608$ for small times $\hat{t} \leq 10^{-1}$. Since the response function is almost constant for small $\hat{t}$, one finds from Eq. (3.44) that

$$\hat{G}(\hat{t}) = \exp\left\{-C_{\rm gauss}\hat{t}^{4/3}\right\} \text{ for } \hat{t} \leq 10^{-1} \ . \tag{3.46}$$

with $C_{\rm gauss} = 9\bar{\nu}/4 \approx 0.3619$. In Fig. 1 the numerical solutions for the scaling functions $\hat{\nu}(\hat{t})$ and $\hat{G}(\hat{t})$ are depicted, as well as the results from the Gaussian approximation (3.46).

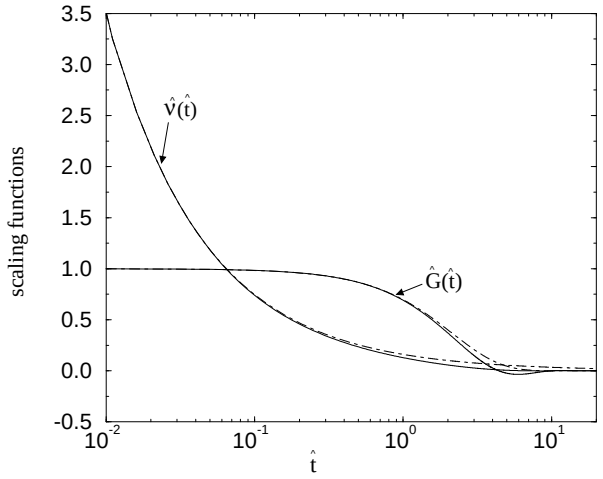

FIG. 1. Scaling functions for the generalized surface tension $\hat{\nu}(\hat{t})$ and response function $\hat{G}(\hat{t})$ vs. the scaling variable $\hat{t} = \lambda(D/\nu)^{1/2}k^{3/2}t$. The point–dashed line represents the Gaussian approximation, Eq. (3.46), for the response function, which is obtained from the analysis of the mode coupling equations at small times.

Truncated correlation function in real space. Another quantity, which is easily accessible by numerical simulations, is the *truncated* correlation function in real space,

$$C(x,t) = \int_{-\infty}^{\infty} \frac{dk}{2\pi} 2\left[1 - e^{ikx}\right] C(k,t) = \frac{D}{\nu} x F\left(\frac{\lambda\sqrt{D/\nu}\, t}{x^{3/2}}\right) , \qquad (3.47)$$

where $F(0) = 1$ since $G(0) = 1$. Conforming to the definition in Eq. (1.11) one gets $A = D/\nu$. The universal scaling function $F(\xi)$ and is shown in Fig. 2.

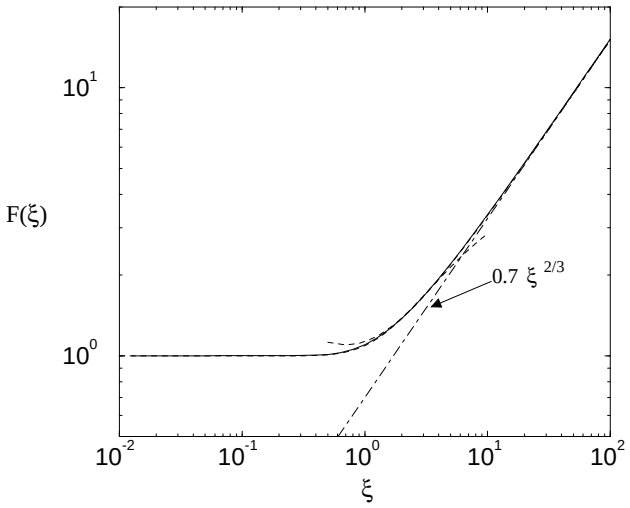

FIG. 2. Scaling function $F(\xi)$ for the truncated correlation function in real space versus the scaling variable $\xi = \lambda A^{1/2}t/x^{3/2}$. The empirical forms, Eq. (3.50), are shown as the dashed curves. The dimensionless coupling constant can be read off from the crossover point of $F(\xi)$.

The dimensionless argument of F has the form demanded by Eq. (1.11) with $z = 3/2$. The dimensionless coupling constant can be read off from the crossover point of $F(\xi)$ (see Fig. 2); we obtain $g^* = 0.87$. This result can be checked more precisely in simulations by directly looking at the scaling amplitudes. Our work thus predicts that if

$$C(x, t = 0) = Ax \ , \qquad (3.48)$$

then

$$C(x = 0, t) = 0.70(\lambda A^2 t)^{2/3} \ . \qquad (3.49)$$

The numerical error is less than $\pm 1\%$. The amplitude 0.70 ± 0.1, extracted from the mode coupling equations, agrees rather well with results from numerical simulations, which find an amplitude of 0.712 ± 0.003 [28] and 0.725 ± 0.005 [29], respectively. In Ref. [29] a empirical form for $F(\xi)$ has been given, which fits the data from the numerical simulation quite well. We find that the mode–coupling result is also quite well approximated by the same empirical forms (dashed curves in Fig. 2)

$$F(\xi) = \begin{cases} 1 + 4.22 \exp\left\{-3.82\xi^{3/2}\right\} & \text{for } \xi \le \xi_0, \\ 0.7\xi^{2/3} + 0.43\xi^{-2/3} & \text{for } \xi \ge \xi_0, \end{cases} \qquad (3.50)$$

where $\xi_0 \approx 2.5$ (see the dashed curves in Fig. 2), but with somewhat different numerical values for the coefficients. Note that the dashed curves are almost indistinguishable from the solid line; in order to make the dashed curves visible we have plotted the asymptotic forms in Eq. 3.50 for values smaller and larger than ξ_0, respectively. In

summary, the mode coupling result for the scaling function $F(\xi)$ agrees with the results from numerical simulation [28,29] within a few percent.

Finite size effects. Note that the above results are valid for very large systems in the *steady state*. Transient behaviors such as the growth of interfacial width starting from flat initial conditions may well be more complicated [39]. They may also be computed using the mode-coupling theory (with Fourier–Laplace transform to incorporate the initial conditions; however, the procedure becomes more cumbersome.

Nevertheless, we can say something about the behavior of systems of finite size L already on the basis of our results for the steady state. In principle, the correlation function and response function are now explicitly L–dependent. They may be described in terms of $D_L(k,\omega) \sim \nu_L(k,\omega) \sim L^{1/2} f(\hat{\omega}, kL)$, where f is now the solution of a two variable integral equation with the initial condition $D_{L=a}(k,\omega) = D$ (the bare value) and similarly for ν. In this way, one would obtain the explicit *functional* renormalization of various quantities as we look at larger length scales L. The flow behavior of D and ν described by usual recursion relations are recovered from the L dependence of $D_L(k=0,\omega=0)$ and $\nu_L(k=0,\omega=0)$. The asymptotic form $D_L \sim \nu_L \sim L^{1/2}$ is of course the expected one given the exponents χ and z [40]. Here we want to emphasize that the self-consistent equations provide a connection between the microscopic and macroscopic (renormalized) theory.

If the flow of these functions is already well advanced, i.e., for times much larger than the initial time $t = 0$, where the interface was absolutely flat, our results for the steady state can also be used to get approximate results for the "transient behavior"of a finite size system. Note that with "transient behavior" we are not referring to the transients starting out from an absolutely flat interface, but to transient behavior after some initial relaxation.

The interface width in a system of finite size L is defined by

$$w_L^2(t) = \left\langle [h(x,t) - h(x,0)]^2 \right\rangle \Big|_L \ . \tag{3.51}$$

Upon assuming that the spectrum of the height function is only slightly modified by finite size effects (and/or after some initial transient), the interface width can be approximated in terms of the correlation function in the steady state

$$\begin{aligned} w_L^2(t) &= 2\int_{-\infty}^{+\infty} \frac{d\omega}{2\pi} \left(1 - e^{i\omega t}\right) 2\int_{2\pi/L}^{+\infty} \frac{dk}{2\pi} C(k,\omega) \\ &= \frac{4D}{\nu} \int_{2\pi/L}^{+\infty} \frac{dk}{2\pi} \frac{1}{k^2} \left[1 - G(k,t)\right] \end{aligned} \tag{3.52}$$

for periodic boundary conditions. Inserting the scaling laws Eqs. (3.37)–(3.40) for the correlation functions one finds

$$w_L^2(t) = \frac{D}{\nu} L f(\tilde{\tau}) \ , \tag{3.53}$$

where $\tilde{\tau} = \lambda\sqrt{\frac{D}{\nu}} L^{-3/2} t$ and

$$f(\tilde{\tau}) = \frac{2}{\pi} \int_{2\pi}^{\infty} dx x^{-2} \left[1 - G(\tilde{\tau} x^{3/2})\right] \ . \tag{3.54}$$

Asymptotically one gets

$$w_L^2(t) = \begin{cases} C_L^2 L & \text{for } t \to \infty \\ C_t^2 t^{2/3} & \text{for } t \to 0 \end{cases} . \tag{3.55}$$

Just as in the discussion of the steady state correlation function one can define an universal amplitude ratio by

$$R = \frac{C_t}{(\lambda C_L^4)^{1/3}} \ , \tag{3.56}$$

and rewrite the scaling law in terms of this ratio

$$w_L(t) = C_L \sqrt{L} W(\tau) \ , \tag{3.57}$$

where $\tau = \lambda C_L t L^{-3/2}$, $C_L^2 = f(\infty) D/\nu$ with $f(\infty) \approx 0.101$. The scaling function $W(\tau)$, shown in Fig. 3, has the following asymptotic behavior

$$W(\tau) = \begin{cases} 1 & \text{for } \tau \to \infty \\ R\tau^{1/3} & \text{for } \tau \to 0 \end{cases} . \tag{3.58}$$

The ratio R is found to be $R = 3.8$, which is in reasonable agreement with $R_{\rm exp} = 3.45 \pm 0.05$ found in numerical simulations [30].

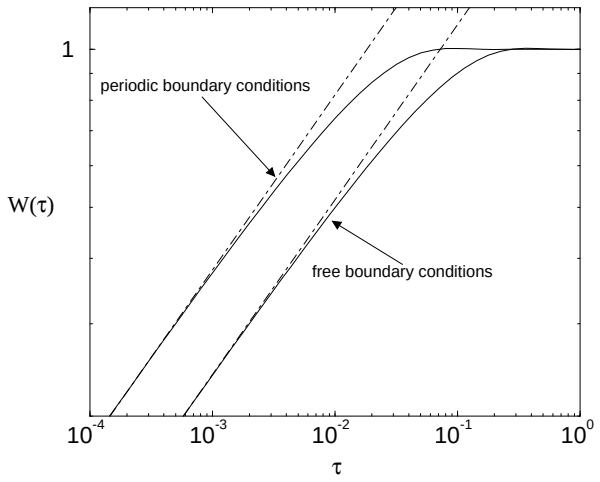

FIG. 3. Scaling function $W(\tau)$ for the interface width in a system of finite size L for periodic boundary conditions and free boundary conditions, respectively. The dashed lines are approximation for small scaled times $\tau = \lambda C_L t L^{-3/2}$, $W(\tau) \approx 3.8\tau^{1/3}$ for periodic boundary conditions and $W(\tau) \approx 2.4\tau^{1/3}$ for free boundary conditions.

If one uses free instead of periodic boundary conditions, one has to replace the lower bound of the integral in Eqs. (3.52) and (3.54) by π. The resulting scaling function for the interface width is also shown in Fig. 3, and we find, as already noted in Ref. [30], that the asymptotic behavior at small times is given by $W(\tau) = R^f \tau^{2/3}$ with $R^f = R/2^{2/3} \approx 2.4$.

D. Vertex corrections

As we have seen in the preceding section mode coupling theory is equivalent to a self–consistent formulation of the perturbation series, where all propagator renormalizations are taken into account, but vertex corrections have been neglected. Nevertheless, there is quite an excellent agreement of the mode coupling results with numerical simulations [28]. It seems that there is some hidden small parameter, which remains to be identified. In this section we address this problem and analyze the magnitude of the vertex corrections.

It is known that the KPZ equation is invariant under a Galilean transformation of the form

$$h'(\mathbf{x},t) = h(\mathbf{x}+\lambda\mathbf{v}t,t) + \mathbf{v}\cdot\mathbf{x}\ , \tag{3.59}$$

$$\widetilde{h}'(\mathbf{x},t) = \widetilde{h}(\mathbf{x}+\lambda\mathbf{v}t,t)\ , \tag{3.60}$$

corresponding to an infinitesimal tilt $\mathbf{v}$ of the surface. This invariance leads to Ward identities, connecting the two– and three–point vertex functions [2], which imply that the nonlinearity λ is not renormalized, and that there is an exponent identity $\chi + z = 2$.

Since the Ward identities relate the three–point with the two–point vertex functions one may hope that they also give some information on the magnitude of the vertex functions. Recently, it has been shown by Lebedev and L'vov [41] that the KPZ equation is invariant under the generalized Galilean transformation

$$h'(\mathbf{x}',t) = h(\mathbf{x},t) + \frac{\partial\boldsymbol{\zeta}}{\partial t}\cdot\mathbf{x}'\,, \tag{3.61}$$

$$\widetilde{h}'(\mathbf{x}',t) = \widetilde{h}(\mathbf{x},t)\,, \tag{3.62}$$

with $\mathbf{x}' = \mathbf{x} - \lambda\boldsymbol{\zeta}$, and where $\boldsymbol{\zeta}$ is an arbitrary function of time but not of coordinates $\mathbf{x}$. Since the generating functional for the vertex functions $\Gamma[\widetilde{h},h]$ is invariant with respect to the above transformation, one finds the following Ward identity

$$\int_{\mathbf{k}}\int dt\left[\lambda\mathbf{k}\cdot\boldsymbol{\zeta}\left\{\frac{\delta\Gamma}{\delta h(\mathbf{k},t)}h(\mathbf{k},t) + \frac{\delta\Gamma}{\delta\widetilde{h}(\mathbf{k},t)}\widetilde{h}(\mathbf{k},t)\right\} + \frac{\delta\Gamma}{\delta h(\mathbf{k},t)}\frac{\partial\boldsymbol{\zeta}}{\partial t}\cdot\frac{\partial}{\partial\mathbf{k}}\delta^{(d)}(\mathbf{k})\right] = 0\ . \tag{3.63}$$

Taking functional derivatives of the above equation with respect to $\widetilde{h}(-\mathbf{q}_1,-\mu_1)$ and $h(-\mathbf{k}_1,-\omega_1)$, then taking the limit $h,\widetilde{h}\to 0$, and recalling the definition of the vertex functions, we obtain the following Ward identity

$$\begin{aligned} i\omega\lim_{\mathbf{k}\to 0}\frac{\partial}{\partial\mathbf{k}}\Gamma_{1,2}(\mathbf{q}_1,\mu_1\mid\mathbf{k}_1,\omega_1;\mathbf{k},\omega) \\ = \lambda\Big\{\mathbf{q}_1\Gamma_{1,1}(\mathbf{q}_1,\mu_1+\omega\mid\mathbf{k}_1,\omega_1) \\ +\mathbf{k}_1\Gamma_{1,1}(\mathbf{q}_1,\mu_1\mid\mathbf{k}_1,\omega_1+\omega)\Big\}\ . \end{aligned} \tag{3.64}$$

Similarly, by taking derivatives of Eq. (3.63) with respect to $\widetilde{h}(-\mathbf{q}_1,-\mu_1)$ and $\widetilde{h}(-\mathbf{q}_2,-\mu_2)$, we get

$$\begin{aligned} i\omega\lim_{\mathbf{k}\to 0}\frac{\partial}{\partial\mathbf{k}}\Gamma_{2,1}(\mathbf{q}_1,\mu_1;\mathbf{q}_2,\mu_2\mid\mathbf{k},\omega) \\ = \lambda\Big\{\mathbf{q}_1\Gamma_{2,0}(\mathbf{q}_1,\mu_1+\omega;\mathbf{q}_2,\mu_2\mid\cdot) \\ +\mathbf{q}_2\Gamma_{2,0}(\mathbf{q}_1,\mu_1;\mathbf{q}_2,\mu_2+\omega\mid\cdot)\Big\}\,. \end{aligned} \tag{3.65}$$

The general Ward identity reads

$$\begin{aligned} i\omega\boldsymbol{\nabla}_{\mathbf{k}}\Gamma_{m,n+1}(\{\mathbf{Q}_i\}|\{\mathbf{K}_i\};\mathbf{k},\omega)|_{\mathbf{k}=0} \\ = \lambda\sum_{j=1}^{m}\mathbf{q}_j\Gamma_{m,n}(\{\mathbf{Q}_i\}+\omega\mathbf{e}_j|\{\mathbf{K}_i\}) \\ +\lambda\sum_{j=1}^{n}\mathbf{k}_j\Gamma_{m,n}(\{\mathbf{Q}_i\mid\{\mathbf{K}_i\}+\omega\mathbf{e}_j)\ , \end{aligned} \tag{3.66}$$

where we have defined $\{\mathbf{Q}_i\} = \mathbf{q}_1,\mu_1;\ldots;\mathbf{q}_m,\mu_m$, $\{\mathbf{K}_i\} = \mathbf{k}_1,\omega_1;\ldots;\mathbf{k}_n,\omega_n$, and $\{\mathbf{Q}_i\}+\omega\mathbf{e}_j = \mathbf{q}_1,\mu_1;\ldots;\mathbf{q}_j,\mu_j+\omega;\ldots;\mathbf{q}_m,\mu_m$. Inserting the above Ward identities, Eq. (3.64) and Eq. (3.65), into the expression for the vertex correction, we find

$$\begin{aligned} \boldsymbol{\nabla}_{\mathbf{k}}V(\mathbf{K}_+;\mathbf{K})\mid_{\mathbf{k}=0} = \frac{\lambda}{i\omega}\mathbf{q}\Big\{-i\omega+\nu^*(\mathbf{q},\mu_-)-\nu^*(\mathbf{q},\mu_+) \\ -\frac{\nu(\mathbf{q},\mu_+)+\nu^*(\mathbf{q},\mu_+)}{2D(\mathbf{q},\mu_+)}\left[D(\mathbf{q},\mu_-)-D(\mathbf{q},\mu_+)\right]\Big\}\,, \end{aligned} \tag{3.67}$$

where $\mu_\pm = \mu\pm\frac{\omega}{2}$. The first term in the latter equation corresponds to the bare vertex, which is real. The corrections to this bare vertex result from the imaginary part of the frequency dependent surface tension $\nu(\mathbf{k},\omega)$ in the second and third term of Eq. (3.67). In addition, the renormalized vertex contains an imaginary part resulting from the real part of the generalized surface tension and the noise amplitude $D(\mathbf{k},\omega)$.

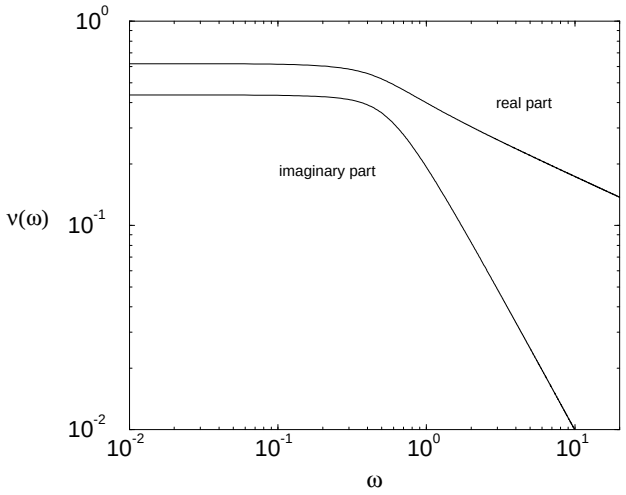

FIG. 4. Scaling function for the real part, $Re\left[\hat{\nu}(\hat{\omega})\right]$, and imaginary part divided by the scaled frequency, $Im\left[\hat{\nu}(\hat{\omega})\right]/\hat{\omega}$, of the generalized surface tension.

Let us first discuss the vertex corrections resulting from the imaginary part of the generalized surface tension. Using the mode coupling results from Section III C, one can calculate the real and imaginary part of $\nu(\mathbf{k},\omega)$, as shown in Fig. 4.

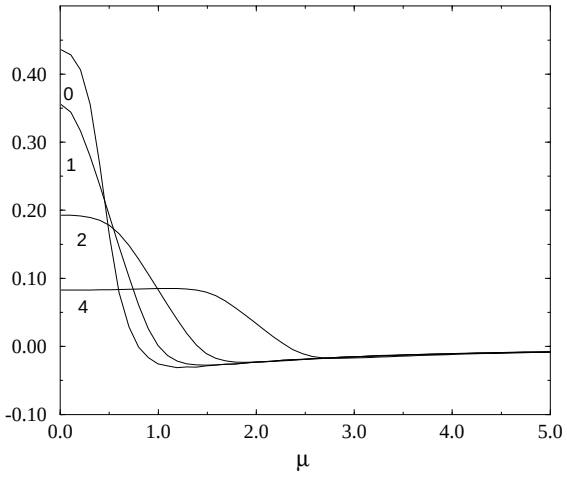

FIG. 5. Real part of the vertex correction versus $\hat{\mu}$, $\mathrm{Im}\left[\hat{\nu}(\hat{\mu}-\frac{\hat{\omega}}{2})-\hat{\nu}(\hat{\mu}+\frac{\hat{\omega}}{2})\right]/\hat{\omega}$. The value of the scaling variable $\hat{\omega}$ is indicated in the graph.

Therefrom one deduces the real part of the vertex corrections

$$Re\left[\boldsymbol{\nabla}_{\mathbf{k}}V(\mathbf{K}_+;\mathbf{K})\mid_{\mathbf{k}=0}\right]+\lambda\mathbf{q}= \\ -\lambda\mathbf{q}Im\left[\hat{\nu}(\hat{\mu}-\tfrac{\hat{\omega}}{2})-\hat{\nu}(\hat{\mu}+\tfrac{\hat{\omega}}{2})\right]/\hat{\omega}\ , \tag{3.68}$$

where $\hat{\mu}=\mu/\bar{\lambda}\nu q^{3/2}$ and $\hat{\omega}=\omega/\bar{\lambda}\nu q^{3/2}$. As can be inferred from Fig. 5 the vertex corrections may be as large as 40% at certain values of the external frequencies. If we take the integral over all frequencies as a measure of the vertex correction, however, we find that it is only of the order of a few percent or even less.

E. Vertex corrections from the two–loop contributions

In this subsection we study the vertex corrections resulting from two–loop diagrams in Lorentzian approximation. With the ansatz $\nu(q)=\nu(q,\omega=0)=\nu_{\mathrm{lor}}(\lambda/\sqrt{2\pi})q^{z-2}$ the mode–coupling equations in Lorentzian approximation read (note that $z=3/2$)

$$\nu_{\mathrm{lor}}^2=\frac{1}{2}\int_{-\infty}^{+\infty}dy\frac{1}{y_+^{3/2}+y_-^{3/2}} \tag{3.69}$$

where $y_\pm=\frac{1}{2}\pm y$. This gives $\nu_{\mathrm{lor}}^2\approx 1.955$. Next we take into account vertex corrections from the two–loop diagrams. We have seen in section II C that the two–loop contributions to $\nu(q,0)$ can be split into a propagator renormalization and a vertex correction. The former is already taken into account in the self–consistency scheme of mode coupling theory. Hence, in Lorentzian approximation one may extend the mode–coupling approach in the following way

$$\nu(q)=\frac{\lambda^2}{2}\int_p\frac{1+V^{(1)}(p/q)}{\nu(q_+)q_+^2+\nu(q_-)q_-^2}\ ; \tag{3.70}$$

with

$$V^{(1)}(y)=\frac{2y-1}{\nu_{\mathrm{lor}}^2}\int dx\frac{\frac{1}{2}+y+x}{\left[\tilde{y}_+^{\frac{3}{2}}+\tilde{y}_-^{\frac{3}{2}}\right]\left[\tilde{y}_-^{\frac{3}{2}}+y_+^{\frac{3}{2}}+|x|^{\frac{3}{2}}\right]}\ , \tag{3.71}$$

where $\tilde{y}_\pm=|\frac{1}{2}\pm y\pm x|$ and $y_\pm=|\frac{1}{2}\pm y|$. As can be inferred from Fig. 6, the vertex corrections $V^{(1)}$ are not at all small as compared to the bare term 1. They vary from about -100% to $+100\%$ as a function of the ratio of the external momenta q and p.

However, by inserting this vertex correction in the extended mode coupling equation, Eq. (3.70), one finds $\nu_{\mathrm{lor}}^2\approx 2.044$, which is merely less than 5% larger than the value obtained with the bare vertex. In addition, the correction tends to increase the amplitude ratio calculated in section III C towards the value obtained from numerical simulations. This result clearly explains why mode coupling theory has been so successful in calculating scaling functions for the noisy Bugers equation.

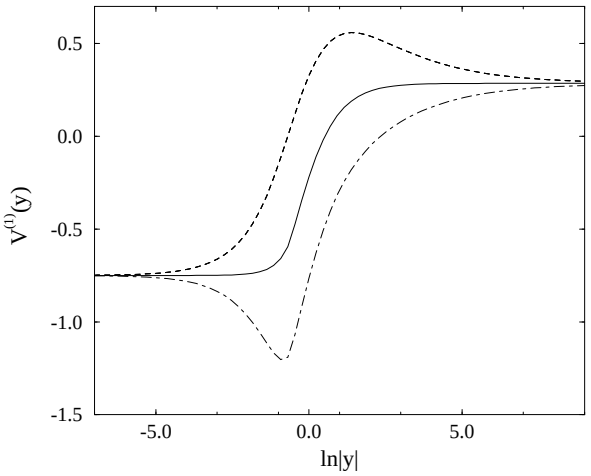

FIG. 6. Vertex correction $V^{(1)}(y)$ from two-loop diagrams as a function of $\ln|y|$: dashed curve: $y < 0$, dot-dashed curve: $y > 0$. The solid line represents the average $\bar{V}^{(1)}(y) = \left[V^{(1)}(y) + V^{(1)}(-y)\right]/2$.

It still remains a puzzle to us, however, that the vertex correction itself constitutes such a large correction to the bare vertex of the order of $\pm 100\%$, while its effect on the correlation function is much less. Future investigations may concentrate on the extension of the two–loop vertex correction to higher orders, e.g. by including all ladder diagrams to the three–point vertex function, which may give us further insight in the validity and accuracy of the fairly simple mode–coupling approach.

IV. SUMMARY AND CONCLUSIONS

In this paper we have investigated the noisy Burgers equation using dynamical renormalization group and mode–coupling techniques. The renormalization group results show that there appears no singular two–loop contribution to the height–height correlation function. Upon including the two–loop vertex corrections into the mode–coupling approach we were able to show that their effect on the result for the correlation function is approximately 5%, whereas the vertex corrections themselves are quite large. We suppose that this overestimates the actual vertex correction. In order to go beyond the two–loop vertex corrections one should possibly use an additional suitable resummation of the vertex correction, e.g., write down a "Bethe–Salpeter" type of equation for the vertices representing all ladder diagrams contributing to the three–point vertex functions. We leave this problem, and conceivable further extensions, for future investigations.

As a complementary estimate for the vertex corrections we have used Ward identities to derive a relation between certain derivatives of the three–point vertex function and the renormalized noise amplitude and surface tension. Again, one finds that the effect of the vertex corrections may be of the order of a few percent.

Based on the above estimates for the vertex corrections, we suppose that mode coupling theory yields very accurate results for the scaling functions, at least for the (1+1)–dimensional KPZ (noisy Burgers) equation. This conclusion is supported by the close agreement of the mode coupling results with those from numerical simulations of finite size systems. It remains unclear, however, whether the mode–coupling approach works as well in the general $(d+1)$–dimensional case, where the two–loop perturbation theory corrections do contain singular contributions.

ACKNOWLEDGMENTS

E.F. and U.C.T gratefully acknowledge support from the Deutsche Forschungsgemeinschaft (DFG) under Contract Nos. Fr. 850/2, SFB 266 and Ta. 177/1, respectively. T.H. is supported by an A. P. Sloan Research Fellowship and an ONR Young Investigator Award.

APPENDIX A: GENERALIZED FLUCTUATION DISSIPATION RELATION

In this appendix we collect several fluctuation dissipation theorems (FDT's), which are of importance for the dynamics of systems described by nonlinear Langevin equations.

Let $\mathcal{T}$ be the time reversal operation: $t \to -t$. Then detailed balance (time inversion symmetry) implies [43] that

$$\mathcal{T} \exp\left[\mathcal{J}_{t_1}^{t_2} - F_{t_1}\right] = \exp\left[\mathcal{J}_{-t_2}^{-t_1} - F_{-t_2}\right] \ , \tag{A1}$$

where $F_t = F[h(t)]$ is the stationary probability distribution function and

$$\mathcal{J}_{t_1}^{t_2}[h,\tilde{h}] = \int dx \int_{t_1}^{t_2} dt \left[\tilde{h}(x,t) D\tilde{h}(x,t) - \tilde{h}(x,t)\left(\frac{\partial h(x,t)}{\partial t} - V(h)\right)\right] , \tag{A2}$$

with

$$V(h) = -D\frac{\delta F}{\delta h} + \frac{\lambda}{2}(\nabla h)^2 \ . \tag{A3}$$

Without loss of generality, one can assume that the field $h(x,t)$ is even or odd under time reversal, that is

$$\mathcal{T} h = \varepsilon h, \quad \varepsilon = \pm 1 \ . \tag{A4}$$

Here h is odd under time reversal. The stationary distribution $P_{\rm st}[h] = e^{-F[h]}$ is characterized by the "free energy"

$$F[h] = \frac{\nu}{2D} \int dx (\nabla h)^2 \ . \tag{A5}$$

The time reversal symmetry implies that

$$\mathcal{T} \widetilde{h}(t) = -\varepsilon \left(\widetilde{h}(-t) - \frac{\delta F[h(-t)]}{\delta h(-t)} \right) \ . \tag{A6}$$

Now one uses the causality property of the response functions, $\langle h(t_1)...h(t_k)\widetilde{h}(\tilde{t}_1)...\widetilde{h}(\tilde{t}_k)\rangle = 0$, if one $\tilde{t}_j \rangle$ all t_i. Then for example

$$\langle h(t)\widetilde{h}(0)\rangle = 0 \text{ for } t < 0 \ . \tag{A7}$$

With the time reversal operation and Eq. (A6) it follows then from Eq. (A7) for $t < 0$ that

$$\left\langle h(-t) \left(\widetilde{h}(0) - \frac{\delta F[h(0)]}{\delta h(0)} \right) \right\rangle = 0 \ . \tag{A8}$$

Upon redefining $t = -t$, one obtains for $t > 0$

$$\langle h(t)\widetilde{h}(0)\rangle = \Theta(t) \left\langle h(t) \frac{\delta F[h(0)]}{\delta h(0)} \right\rangle \ . \tag{A9}$$

The same arguments can be repeated for $\langle h(t_1)...h(t_k)\widetilde{h}(\tilde{t}_1)\rangle$ with $\tilde{t}_1 >$ all t_j. The result is

$$\begin{aligned} &\langle h(t_1)...h(t_k)\widetilde{h}(\tilde{t}_1)\rangle \\ &= \Theta(\tilde{t}_1, \{t_j\}) \left\langle h(t_1)...h(t_k) \frac{\delta F[h(\tilde{t}_1)]}{\delta h(\tilde{t}_1)} \right\rangle \ . \end{aligned} \tag{A10}$$

where $\Theta(\tilde{t}_1, \{t_j\})$ is an obvious generalization of the Θ function. Note that these generalized FDT's are for the cumulants and not for the vertex functions. In particular we get

$$G_{11}(k,t) = \Theta(t) \frac{\nu k^2}{D} G_{02}(k,t) \, . \tag{A11}$$

Further identities can be written down in a completely analogous way [36,43].

APPENDIX B: TWO–LOOP PERTURBATION THEORY FOR THE TWO–POINT VERTEX FUNCTIONS

This appendix comprises the Feynman diagrams to two–loop order for the (1+1)–dimensional Kardar–Parisi–Zhang equation, and the corresponding momentum integrals. The integrations over the internal frequencies have already been performed using the residue theorem.

We start with a list of the contributions to two–loop order to the fully wavevector– and frequency–dependent two–point vertex function $\Gamma_{\tilde{h}h}(q,\omega)$. The other non–vanishing vertex function $\Gamma_{\tilde{h}\tilde{h}}(q,\omega)$ can be calculated in a similar fashion (see Ref. [2]), or simply be obtained via the fluctuation–dissipation theorem (2.8). In writing down the diagrammatic expansion for the dynamic functional one has to take into account restrictions which follow from causality. In section II we have not explicitly included the Jacobian $\mathcal{J}[h] = \mathcal{D}[\eta]/\mathcal{D}[h]$, which depends on the discretization of the Langevin equation (needed to give a proper definition to the path integral). As can be shown quite generally [36], the Jacobian cancels the equal–time contractions of the field h and the response field $\tilde{h}$. Keeping this in mind (or by choosing a discretization with the Jacobian equal to 1), one can omit the Jacobian in the dynamic functional. The Feynman diagrams, which account for the restrictions imposed by causality, are depicted in Fig. 7.

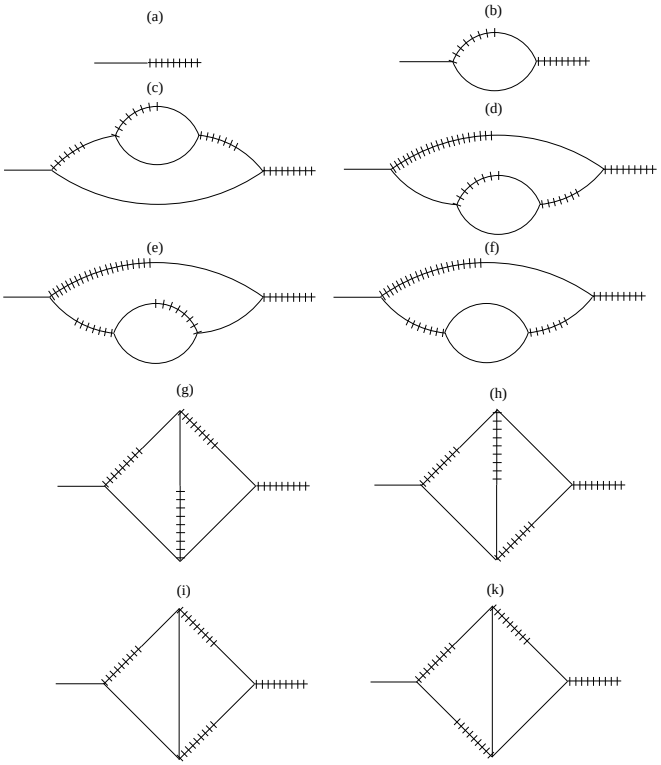

FIG. 7. Feynman diagrams for the two–point vertex function $\Gamma_{\tilde{h}h}(q,\omega)$ to two–loop order.

Introducing the abbreviations $q_\pm = (q/2) \pm p$, $\bar{q}_\pm = (q_-/2) \pm k$, and $\tilde{q}_\pm = q_\pm \pm k$, the corresponding analytical expressions read:

$$\begin{aligned} &\Gamma_{\tilde{h}h}(q,\omega) \ : \\ &(a)+(b) = i\omega + \nu_0 q^2 + \frac{\lambda^2 D_0}{2\nu_0} q^2 \int_p \frac{1}{i\omega + \nu_0 q_+^2 + \nu_0 q_-^2} \ , \end{aligned} \tag{2.1}$$

$$(c) = -\frac{\lambda^4 D_0^2}{2\nu_0^2} q \int_p \frac{q_-^3}{(i\omega + \nu_0 q_+^2 + \nu_0 q_-^2)^2} \int_k \frac{1}{i\omega + \nu_0 q_+^2 + \nu_0 \tilde{q}_+^2 + \nu_0 \tilde{q}_-^2} \ , \tag{2.2}$$

$$(d) = -\frac{\lambda^4 D_0^2}{2\nu_0^2} q \int_p \frac{q_+ q_-^2}{i\omega + \nu_0 q_+^2 + \nu_0 q_-^2} \int dk \, \frac{1}{\nu_0 q_-^2 + \nu_0 \tilde{q}_+^2 + \nu_0 \tilde{q}_-^2} \tag{2.3}$$
$$\times \left[\frac{1}{2\nu_0 q_-^2} + \frac{1}{i\omega + \nu_0 q_+^2 + \nu_0 \tilde{q}_+^2 + \nu_0 \tilde{q}_-^2} \left(1 + \frac{\nu_0 q_-^2 + \nu_0 \tilde{q}_+^2 + \nu_0 \tilde{q}_-^2}{i\omega + \nu_0 q_+^2 + \nu_0 q_-^2} \right) \right] ,$$

$$(e) = -\frac{\lambda^4 D_0^2}{2\nu_0^2} q \int_p \frac{q_+ q_-^2}{2\nu_0 q_-^2 [i\omega + \nu_0 q_+^2 + \nu_0 q_-^2]} \int_k \frac{1}{\nu_0 q_-^2 + \nu_0 \tilde{q}_+^2 + \nu_0 \tilde{q}_-^2} \ , \tag{2.4}$$

$$(f) = \frac{\lambda^4 D_0^2}{2\nu_0^2} q \int_p \frac{q_+ q_-^2}{i\omega + \nu_0 q_+^2 + \nu_0 q_-^2} \int_k \frac{1}{\nu_0 q_-^2 + \nu_0 \tilde{q}_+^2 + \nu_0 \tilde{q}_-^2} \left(\frac{1}{\nu_0 q_-^2} + \frac{1}{i\omega + \nu_0 q_+^2 + \nu_0 \tilde{q}_+^2 + \nu_0 \tilde{q}_-^2} \right) , \tag{2.5}$$

$$(g) = -\frac{\lambda^4 D_0^2}{\nu_0^2} q \int_p \frac{q_+}{i\omega + \nu_0 q_+^2 + \nu_0 q_-^2} \int_k \frac{\tilde{q}_+ k}{[\nu_0 q_-^2 + \nu_0 \tilde{q}_-^2 + \nu_0 k^2][i\omega + \nu_0 \tilde{q}_+^2 + \nu_0 \tilde{q}_-^2]} \tag{2.6}$$
$$\times \left(1 + \frac{2\nu_0 q_-^2}{i\omega + \nu_0 q_+^2 + \nu_0 \tilde{q}_-^2 + \nu_0 k^2} \right) ,$$

$$(h) = -\frac{\lambda^4 D_0^2}{\nu_0^2} q \int_p \frac{q_-}{i\omega + \nu_0 q_+^2 + \nu_0 q_-^2} \int_k \frac{\tilde{q}_+ k}{[i\omega + \nu_0 \tilde{q}_+^2 + \nu_0 \tilde{q}_-^2][i\omega + \nu_0 q_+^2 + \nu_0 \tilde{q}_-^2 + \nu_0 k^2]} \ , \tag{2.7}$$

$$(i) = -\frac{\lambda^4 D_0^2}{\nu_0^2} q \int_p \frac{q_-}{i\omega + \nu_0 q_+^2 + \nu_0 q_-^2} \int_k \frac{\tilde{q}_+ \tilde{q}_-}{[i\omega + \nu_0 \tilde{q}_+^2 + \nu_0 \tilde{q}_-^2][i\omega + \nu_0 q_+^2 + \nu_0 \tilde{q}_-^2 + \nu_0 k^2]} \tag{2.8}$$
$$- \frac{\lambda^4 D_0^2}{\nu_0^2} q \int_p \frac{q_+}{i\omega + \nu_0 q_+^2 + \nu_0 q_-^2} \int_k \frac{\tilde{q}_+ \tilde{q}_-}{[\nu_0 q_-^2 + \nu_0 \tilde{q}_-^2 + \nu_0 k^2][i\omega + \nu_0 \tilde{q}_+^2 + \nu_0 \tilde{q}_-^2]}$$
$$\times \left(1 + \frac{2\nu_0 q_-^2}{i\omega + \nu_0 q_+^2 + \nu_0 \tilde{q}_-^2 + \nu_0 k^2} \right) ,$$

$$(j) = \frac{\lambda^4 D_0^2}{\nu_0^2} q \int_p q_+ q_- \int_k \frac{\tilde{q}_+}{[\nu_0 q_-^2 + \nu_0 \tilde{q}_-^2 + \nu_0 k^2][i\omega + \nu_0 \tilde{q}_+^2 + \nu_0 \tilde{q}_-^2][i\omega + \nu_0 q_+^2 + \nu_0 \tilde{q}_-^2 + \nu_0 k^2]} \ . \tag{2.9}$$

* Present address: Department of Physics – Theoretical Physics, University of Oxford, 1 Keble Road, Oxford OX1 3NP, U.K.

1 M. Kardar, G. Parisi, and Y.-C. Zhang, Phys. Rev. Lett. **56**, 889 (1986); E. Medina, T. Hwa, M. Kardar, and Y.-C. Zhang, Phys. Rev. A **39**, 3053 (1989).

2 E. Frey and U.C. Täuber, Phys. Rev. E **50**, 1024 (1994).

3 M. Lässig, Nucl. Phys. B ?? (1996).

4 For a recent review, see e.g.: T. Halpin-Healy and Y.-C. Zhang, Phys. Rep. **254**, 215 (1995).

5 T. Ala-Nissila, T. Hjelt, J.M. Kosterlitz, and O. Venäläinen, J. Stat. Phys. **72**, 207 (1993).

6 J.P. Doherty, M.A. Moore, J.M. Kim, and A.J. Bray, Phys. Rev. Lett. **72**, 2041 (1994).

7 J-P. Bouchaud and M.E. Cates, Phys. Rev. E **47**, 1455 (1993); *ibid.* **48**, 635 (E) (1993).

8 Y. Tu, Phys. Rev. Lett. **73**, 3109 (1994).

9 M.A. Moore, T. Blum, J.P. Doherty, M. Marsili, J-P. Bouchaud, and P. Claudin, Phys. Rev. Lett. **74**, 4257 (1995).

10 T. Halpin-Healy, Phys. Rev. A **42**, 711 (1990).

11 T. Nattermann and H. Leschhorn, Europhys. Lett. **14**, 603 (1991).

12 U.C. Täuber and E. Frey, Phys. Rev. E **51**, 6319 (1995).

13 D. Forster, D. R. Nelson, and M. J. Stephen, Phys. Rev. A **16**, 732 (1977).

14 D. A. Huse, C. L. Henley, and D. S. Fisher, Phys. Rev. Lett. **55**, 2924 (1985); M. Kardar and Y.-C. Zhang, Phys. Rev. Lett. **58**, 2087 (1987); for a recent review, see: D. S. Fisher and D. A. Huse, Phys. Rev. B **43**, 10728 (1991).

15 T. Hwa and D.S. Fisher, Phys. Rev. B **49**, 3136 (1994).

16 T. Sun and M. Plischke, Phys. Rev. E **49**, 5046 (1994); T. Sun, Phys. Rev. E **51**, 6316 (1995).

17 G. Sivashinsky, Acta Astronautica **4**, 1177 (1977); Y. Kuramoto, Suppl. Prog. Theor. Phys. **64**, 346 (1978).

18 K. Sneppen, J. Krug, M.H. Jensen, C. Jayaprakash, and T. Bohr, Phys. Rev. A **46**, R7351 (1992).

19 C.C. Chow and T. Hwa, Physica D 84, 494 (1995).

20 V.S. L'vov and I. Procaccia, Phys. Rev. Lett. **69**, 3543 (1992); I. Procaccia, M.H. Jensen, V.S. L'vov, K. Sneppen, and R. Zeitak, Phys. Rev. A **46**, 3220 (1992).

21 L. Golubović and Z.-G. Wang, Phys. Rev. E **49**, 2567 (1994).

22 A. Kashuba, Phys. Rev. Lett. **73**, 2264 (1994).

23 J. Krug and H. Spohn, Europhys. Lett. **8**, 219 (1989).

24 H. van Beijeren, R. Kutner, and H. Spohn, Phys.

Rev. Lett. **54**, 2026 (1985); H. K. Janssen and B. Schmittmann, Z. Phys. B **63**, 517 (1986).

[25] I. Ispolatov, P.L. Krapivsky, and S. Redner, Phys. Rev. E **52**, 2540 (1995).

[26] H.C. Fogedby, A.B. Eriksson, and L.V. Mikheev, Preprint (1995).

[27] T. Hwa and E. Frey, Phys. Rev. A **44**, R7873 (1991).

[28] J. Krug, P. Meakin, and T. Halpin-Healy, Phys. Rev. A **45**, 638 (1992).

[29] L.-H. Tang, J. Stat. Phys. **67**, 819 (1992).

[30] J.G. Amar and F. Family, Phys. Rev. A **45**, R3373 (1992); *ibid.* **45**, 5378 (1992).

[31] W. Götze, in: *Liquids, Freezing, and the Glass Transition* , ed. J.P. Hansen, D. Levesque, and J. Zinn-Justin (North Holland, 1991); W. Götze and L. Sjögren, Rep. Prog. Phys. **55**, 241 (1992).

[32] K. Kawasaki, Ann. Phys. (N.Y.) **61**, 1 (1970).

[33] E. Frey and F. Schwabl, Adv. Phys. **43**, 577 (1994).

[34] K. Kawasaki, in: *Phase Transitions and Critical Phenomena*, Vol 5a, ed. C. Domb and M.S. Green (Academic Press, New York, 1976).

[35] A.S. Monin and A.M. Yaglom, *Statistical Fluid Mechanics* (MIT, Cambridge, MA, 1975), Vol. 2, Sec. 19.6,, p295.

[36] H.K. Janssen, Z. Phys. B **23**, 377 (1976); R. Bausch, H.K. Janssen, and H. Wagner, Z. Phys. B **24**, 113 (1976).

[37] C. de Dominicis, Nuovo Cim. Lett. **12**, 567 (1975); J. Phys. (Paris) **37**, Colloq. C-247 (1976).

[38] P.C. Martin, E.D. Siggia, and H.H. Rose, Phys. Rev. A **8**, 423 (1973).

[39] See, e.g, F. Family, Physica A **168**, 561 (1990); and references therein.

[40] D. E. Wolf and L.-H. Tang, Phys. Rev. Lett. **65**, 1591 (1990).

[41] V.S. L'vov and V.V. Lebedev, Europhys. Lett. **22**, 419 (1993); V.V. Lebedev and V.S. L'vov, Phys. Rev. E **49**, R959 (1994).

[42] R. Graham, in: *Springer Tracts in Modern Physics*, Vol. 66, (Springer-Verlag, Berlin, 1973).

[43] see H.K. Janssen, in: *Lecture Notes in Physics 104, Dynamic Critical Phenomena and Related Topics*, ed. C.P. Enz, (Springer-Verlag, Berlin, 1979).